Journal of the Korean Physical Society, Vol. 59, No. 2, August 2011, pp. 1581∼1584

Method Developing and Testing for Inelastic Scattering Measurements at the GELINA Facility

A. Plompen,* N. Nankov, C. Rouki and M. Stanoiu

European Commission, Joint Research Centre, Institute for Reference Materials and Measurements (IRMM), Retieseweg 111, 2440 Geel, Belgium

C. Borcea, D. Deleanu and A. Negret

"Horia Hulubei" National Institute for Physics and Nuclear Engineering, Bucharest - Magurele 070125, Romania

P. Dessagne, M. Kerveno, G. Rudolf and J. C. Thiry

Institut Pluridisciplinaire Hubert Currien (IPHC),
Centre national de la recherche scientifique (CNRS)/Département Recherches Subatomiques-Université de Strasbourg, CNRS/Institut national de physique nucléaire et de physique des particules, 23 rue du Loess, Strasbourg, France

M. Mosconi and R. Nolte

Physikalisch Technische Bundesanstalt (PTB), Bundesallee 100, D-38116 Braunschweig, Germany

(Received 26 April 2010)

Accurate inelastic scattering measurements are of interest to improving modelling and simulation of advanced reactor systems through better nuclear data (OECD-NEA, High priority request list for nuclear data http://www.nea.fr/html/dbdata/hprl/). Two setups are available at IRMM for measurements of inelastic scattering with the $(n, n'\gamma)$-technique. The first the GAINS gamma-array for inelastic neutron scattering at a 200 m station consists of eight high purity germanium detectors, has high incident neutron energy resolution and is therefore tailored for inelastic scattering measurements. The second, at a 30 m station was developed by IPHC with the purpose of studying actinides for the Th/U cycle and emphasizing besides $(n, n'\gamma)$ also $(n, 2n\gamma)$ reactions. In the recent past a number of efforts were started to investigate the uncertainties and corrections required to obtain reliable results and to investigate the limits of accuracy of this technique. A joint effort is described that has led to an improved understanding of the fission chambers used. In particular, the important corrections to the efficiency for fission fragment loss were investigated.

PACS numbers: 29.40.-n, 28.20.-v
Keywords: Neutron inelastic scattering, Fluence measurement
DOI: 10.3938/jkps.59.1581

I. INTRODUCTION

At IRMM two measurement setups are currently devoted to the study of $(n, xn\gamma)$-cross sections. One is called GAINS for isotopes of structural materials, coolants and inert fuel components. The other setup is developed by IPHC for isotopes of actinides. Both make use of the GELINA neutron time-of-flight facility. GAINS is located on flight path 3 at 200 m from the source. The IPHC setup is on flight path 16 at 30 m from the source. The purpose of both arrangements is to improve the knowledge on inelastic and $(n, 2n)$ scattering cross sections which are of interest to the development of future nuclear power plants using Generation-IV reactors. Ongoing experimental work with these arrays is reported elsewhere in these proceedings [1–3], while details about the GELINA time-of-flight facility may be found in Refs. 4 and 5.

Since target uncertainties for many of these cross sections are very tight [6] it is important to investigate the limits of accuracy that may be achieved. The present paper investigates the important aspects of our method of fluence normalization. This work impacts results reported earlier. In addition, we are in the process of re-evaluating our method for the determination of the gamma detection efficiency [7].

II. THE EXPERIMENTAL ARRANGEMENT

1. Principle

For brevity we will not here repeat all the experimental details pertinent to these measurements. Instead we

*E-mail: arjan.plompen@ec.europa.eu

refer the interested reader to earlier publications ([3] and references therein) and to the contributions to this conference concerning the actinides and ^{28}Si [1,2]. For the present purpose it is sufficient to recall that a well-defined beam of neutrons passes first a fission chamber and then, within a distance of less than 1.5 m the sample under study. Both the sample and the fission deposits are perpendicular to the beam. The active deposit(s) of the fission chamber are larger than the beam and in the preferred approach also the diameter of the sample is larger than the beam. Thus neutrons passing the normalization instrument, a fission chamber with deposits of highly enriched ^{235}U, also pass the sample requiring only minor corrections for attenuation of the beam between the deposit(s) and the sample. The sample is viewed by either four planar (IPHC setup) or eight single-ended coaxial (GAINS) detectors.

The starting point for each analysis is the determination of the differential cross section (left hand side of Eq. (1)) for a gamma-ray detected at the nominal angle θ_i and for a neutron energy E_k (i labels the different detectors, k the energy bin).

$$\frac{d\sigma}{d\Omega}(\theta_i, E_k) = \frac{1}{4\pi}\frac{Y_i(E_k)}{Y_{\mathrm{FC}}(E_k)}\frac{\epsilon_{FC}}{\epsilon_i}\frac{t_{\mathrm{n}}}{t_{\mathrm{s}}}\frac{A_{\mathrm{s}}}{A_{\mathrm{n}}}\frac{1}{c_{\mathrm{ms}}}\sigma_{\mathrm{n}}(E_k). \quad (1)$$

The net gamma-ray yields are denoted by $Y_i(E_k)$, the number of fission counts above threshold is given by $Y_{\mathrm{FC}}(E_k)$, the peak efficiency for a specific gamma-ray is given by ϵ_i, the efficiency for observing a fission event above the amplitude threshold is ϵ_{FC}, the mass areal density of the isotope (here ^{235}U) used for the normalization is t_n, the mass areal density for the isotope under study is t_s, the respective mass numbers are A_n and A_s, c_{ms} accounts for multiple scattering. The cross section used for normalization $\sigma_n(E_k)$ is taken from the standards evaluation for the $^{235}U(n, F)$ reaction [8]. For the energy range considered, 0.3 to 20 MeV, it is known to better than a percent, and the most easy to use of all standard cross sections. The normalization accuracy is thus determined primarily by counting statistics Y_{FC}, the knowledge of the efficiency ϵ_{FC} and the ^{235}U mass per unit area t_n. The latter two will be discussed in more detail.

2. The efficiency ϵ_{FC}

Typical fission amplitude spectra for a simple parallel plate ionization chamber with a ^{235}UF$_4$ deposit of 0.475(2) mg/cm^2, 70 mm diameter and 6.5 mm electrode spacing are shown in Fig. 1. The spectra are shown for positive (forward bias) or negative (reverse bias) high voltage.

The GAINS fission chamber has 8 deposits on five electrodes so that half can be considered forward and the other half reverse biased (Fig. 2 bottom). As evident from Fig. 1 this makes for a more delicate positioning of the threshold since the GAINS spectrum corresponds to

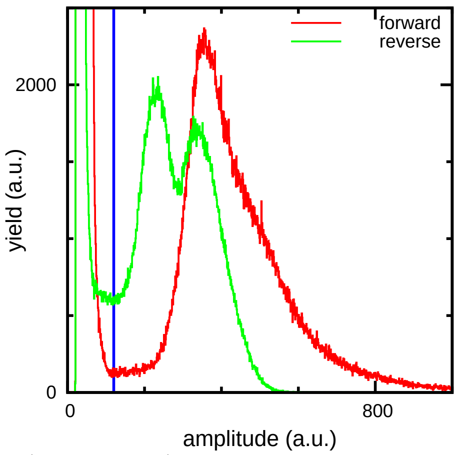

Fig. 1. (Color online) Typical amplitude spectra in case of a single deposit parallel plate configuration as shown in Fig. 2 top.

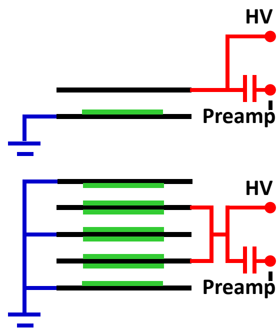

Fig. 2. (Color online) Schematic representation of a single deposit parallel plate configuration (top) and the GAINS multi-electrode parallel plate configuration (6 mm electrode spacing). Deposits indicated in green are evaporated ^{235}UF$_4$ layers on Al backings (black). In the GAINS fission chamber three backings have deposits on both sides.

the sum of the two spectra shown. The threshold should be placed in the linear range between the alpha particle peak at low amplitude and the main fission peak taking care to optimally reject alphas.

To study the impact of the characteristics of the GAINS chamber on the efficiency a number of tests were made with the simple parallel plate configuration shown in the top panel of Fig. 2. The first of these was already shown in Fig. 1.

The fission chamber efficiency is given by

$$\epsilon_{\mathrm{FC}} = \frac{Y_{\mathrm{FC}}}{Y_{\mathrm{FC}} + Y_{\mathrm{A}} + Y_{\mathrm{B}}}, \quad (2)$$

where Y_A corresponds to fission fragments depositing energy in the counter gas but with amplitudes below threshold and Y_B corresponds to fission fragments emitted in the direction of the counter gas but stopped in the deposit.

Experimentally Budtz-Jörgensen *et al.* [9] found for

UF_4 deposits that $Y_B/(Y_{\rm FC} + Y_A + Y_B) = 0.105(7)\ t$, with t the UF_4 thickness in mg/cm^2. In earlier work by our group this effect was not taken into account.

It is tempting to determine Y_A by a linear fit around the threshold determining the area under the fitted line from zero amplitude to the threshold. For the spectra in Fig. 1 this would lead to nonzero fission yields at zero amplitude. However, it may seem counter-intuitive that near zero amplitude fission yields are nonzero. In fact, we have so far used the estimate of Y_A made in reference [10], where the linear fit intercepts the zero-yield axis for positive amplitudes. From the spectra shown in Fig. 1, the region of low fission fragment amplitudes is obscured by the contributions of alphas and/or noise and no conclusions can be drawn about the actual behaviour.

A. Simple model

A simple model allows to demonstrate that one should expect the zero-amplitude yield to be non-zero. Assume a layer of uniform thickness d in which a mono-energetic fission fragment or alpha particle (energy E_0) is born with equal probability for each depth into the layer. Assume further that its direction is isotropic, that the range $R_d(E) = R_d E/E_0$ in the deposit is proportional to the energy and that the same holds for the range in the gas $R_g(E) = R_g E/E_0$. R_d and R_g are constants equal to the range in the deposit material and in the gas for particles with $E = E_0$. Furthermore the charge is taken to be distributed uniformly along the track in the counter gas. The amplitude for a fragment is determined by the product of the charge times the distance travelled to the read-out electrode by integrating over the charge distribution of the track in the counter gas. The spectra for a typical fragment and the configuration of Fig. 2 top with electrode spacing well below the range of a fragment in the gas are shown in Fig. 3. These curves may be obtained by either a straightforward Monte Carlo simulation or by an analytic evaluation. Two contributions to the amplitude spectrum should be considered for both forward and reverse biasing. Fragments striking the opposite electrode will contribute in the same manner to the amplitude spectrum for forward and for reverse bias, since in both cases the distances travelled are the same (common part). However, fragments stopped in the gas will contribute with the largest and the smallest amplitudes for positive bias (forward only), but only with low amplitudes for negative bias (reverse only). In both cases the latter fragments are responsible for the low amplitude spectrum of the respective sums and, as shown, in both cases nonzero yields are to be expected at zero amplitude.

However, there is an important difference. For forward bias the behavior remains linear (although non-zero) for zero amplitude, while for reverse bias an upturn is seen. Another important difference is the magnitude of the yield at low amplitude.

It may be argued that this model has little value given

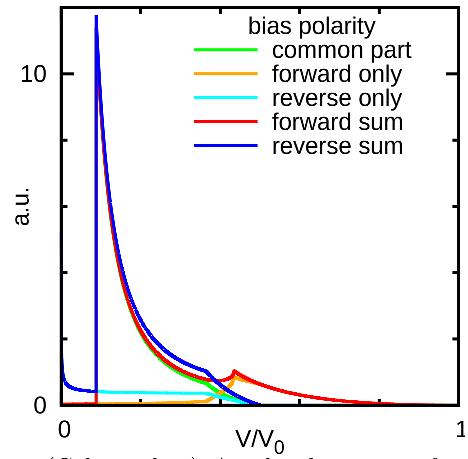

Fig. 3. (Color online) Amplitude spectra for a simple model of a parallel plate ionization chamber.

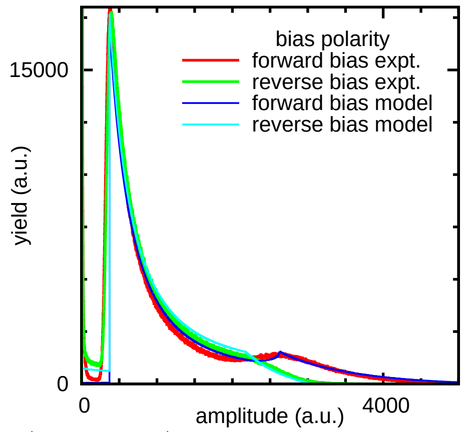

Fig. 4. (Color online) Measured alpha particle amplitude spectra for a parallel plate detector.

the large disparity with the spectra shown in Fig. 1. Figure 4 shows the measured alpha spectra obtained with the configuration shown in the top of Fig. 2 and a high amplification. The model calculations were scaled to show remarkable qualitative agreement. This indicates that the differences observed in Fig. 1 must be due to the spectrum of fission fragment energies and the associated variation in ranges and energy depositions. This was in fact demonstrated by one of us (JCT) by a more elaborate Monte Carlo simulation with GEANT4 including full fission fragment mass and kinetic energy distributions and more realistic stopping powers/ranges.

Taking the model seriously we should expect that Y_A is underestimated for reverse biasing when a linear fit is made. In Fig. 5 we have determined $Y_{\rm FC} + Y_A$ for a repetition of bias reversals using the same fission chamber. Y_A was determined using a linear fit as described above. For normalization to the same number of neutrons a second fission chamber was used that remained unchanged during the exercise. Indeed the reverse bias data of Fig. 1 show a lower mean value for $Y + Y_A$ by as much as 4.4%.

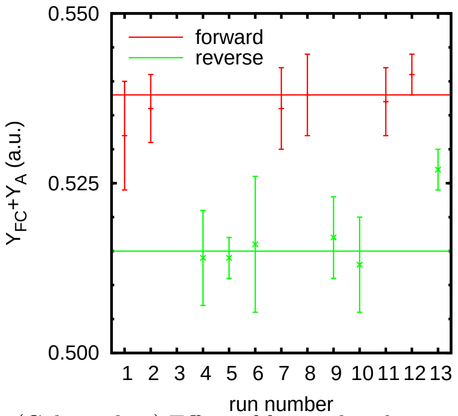

Fig. 5. (Color online) Effect of forward and reverse biasing on the yield $Y_{\mathrm{FC}} + Y_A$.

B. Electrode spacing and biasing polarity

It was also demonstrated for forward biasing that the width of the linear range is determined by the electrode spacing so that increasing the spacing increases this range. We have verified this experimentally by varying the spacing from 5.5 to 6.5 and 7.5 mm for a single deposit fission chamber. In contrast to polarity reversal, varying the electrode spacing has no impact on the value of $Y_{\mathrm{FC}} + Y_A$ when suitably normalized to the same number of neutrons passing the deposit. Thus it may be concluded that the criteria for optimization of the spacing are 1) the discrimination of fission fragments from alphas and 2) the useful range for determining a linear fit.

Finally, it is evident from Fig. 1 that Y_A is much larger for reverse biasing than for forward biasing. In fact, the same study that led to Fig. 5 showed that $Y_A/(Y_{\mathrm{FC}}+Y_A)$ is 3 – 4% for forward and 14 – 16% for reverse biasing.

3. The ^{235}U mass areal density t_n

The mass of ^{235}U of our $^{235}UF_4$ deposits was determined from the total activity and the isotope mass ratio (^{234}U contributes 65% of the activity). The uncertainty on the conversion factor from activity to ^{235}U content was improved from 1.3% to 0.3% by a new isotope ratio measurement. The activity was determined by low-geometry alpha counting prior to configuring the fission chambers with a typical uncertainty of 0.5%. As shown in Fig. 4 the alpha spectra can also be obtained in these chambers by increasing amplification. Thus, it could also be verified that the activity of these deposits was within the uncertainty (1%) in agreement with the original low-geometry activity measurements. Relying on the latter we conclude that the total ^{235}U mass is known to better than 1%.

On the other hand it was shown in Ref. 11 that for these deposits there is a radial profile of the thickness due to the configuration of the evaporator. This profile was quantified by a combination of alpha counting and a Monte Carlo model. Given these data and the fact that the beam diameter is 61 mm while the deposit diameter is 70 mm, it follows that the average mass areal density t_n in the beam is 0.7% higher than the average value.

III. OUTLOOK

The above analysis of the characteristics of a $^{235}UF_4$ parallel plate fission chamber has implications for the efficiency of the GAINS fission chamber and the data that were taken with it. Compared with the efficiency reported in Ref. 10 the actual value is 12 – 15% lower. Thus, taking into account also the effect of the inhomogeneity, cross sections for $(n, xn\gamma)$-reactions reported earlier ([3] and references therein) are lower by 10 – 13%. To quantify this finding further an intercomparison with the PTB primary fluence reference (a recoil proton telescope) and a PTB fission chamber is ongoing. Data were taken at PTB in December 2009 and the analysis is under way.

Concerning the gamma-detection efficiency and the overall accuracy of the methods employed extended ^{152}Eu sources and $^{10}B_4C$ samples with a range of diameters were obtained and will be studied in the near future. In addition, the simulation tools MCNP and GEANT4 for determining gamma-efficiencies were compared and the accuracy of the calibration procedure was verified [7].

REFERENCES

[1] J. Thiry, C. Borcea, P. Dessagne, J. Drohé, E. Jericha, H. Karam, M. Kerveno, A. Koning, A. Negret, A. Pavlik, A. Plompen, P. Romain, C. Rouki, G. Rudolf and M. Stanoiu, *Inter. Conf. on Nucl. Data for Sci. and Techn.-ND2010* (Jeju, Korea, 2010).
[2] A. Negret, C. Borcea and A. J. M. Plompen, *Inter. Conf. on Nucl. Data for Sci. and Techn.-ND2010* (Jeju, Korea, 2010).
[3] C. Rouki, C. Borcea, N. Nankov, A. Negret, A. Plompen and M. Stanoiu, *Inter. Conf. on Nucl. Data for Sci. and Techn.-ND2010* (Jeju, Korea, 2010).
[4] A. Bensussan and J. M. Salomé, Nucl. Instrum. Methods Phys. Res., Sect. A **155**, 11 (1978).
[5] D. Ene *et al.*, Nucl. Instrum. Methods Phys. Res., Sect. A **618**, 54 (2010).
[6] Working Party on International Evaluation Co-operation, *The High Priority Request List for nuclear data (HPRL)* NEA Nuclear Science Commitee (2006). www.nea.fr/dbdata/hprl/.
[7] D. Deleanu *et al.*, Nucl. Instrum. Methods Phys. Res., Sect. A **624**, 130 (2010).
[8] A. Carlson *et al.*, Nucl. Data Sheets **110**, 3215 (2009).
[9] Budtz-Jörgensen and H. Knitter, Nucl. Instrum. Methods Phys. Res., Sect. A **236**, 630 (1985).
[10] L. C. Mihailescu *et al.*, Nucl. Instrum. Methods Phys. Res., Sect. A **531**, 375 (2004).
[11] P. Schillebeeckx *et al.*, Nucl. Instrum. Methods Phys. Res., Sect. A **613**, 378 (2010).